

VOID GROWTH IN FCC AND BCC SINGLE CRYSTALS

J.W. Kysar and Y.X. Gan

Department of Mechanical Engineering, Columbia University, New York, NY 10027

ABSTRACT

The fracture toughness of ductile materials depends upon the ability of the material to resist the growth of microscale voids near a crack tip. Mechanics analyses of the elastic-plastic deformation state around such voids typically assume the surrounding material to be isotropic. However at the microscale, voids exist predominantly within single grains of a polycrystalline material, so it is necessary to account for the anisotropic nature of the surrounding material. Therefore anisotropic slip line theory is employed herein to derive the stress and deformation state around a cylindrical void in a single crystal oriented such that plane strain conditions are admitted from three effective in-plane slip systems. The deformation state takes the form of angular sectors around the circumference of the void. Only one of the three effective slip systems is active within each sector. Each slip sector is further subdivided into smaller sectors within which the stress state is derived. The theory predicts a highly heterogeneous stress and deformation state. Theoretical results will be presented for voids in both face centered cubic and body centered cubic crystals. Experiments and single crystal plasticity finite element simulations of cylindrical voids in single crystals are also discussed. It is shown that the in-plane pressure necessary to activate plastic deformation around a cylindrical void in an anisotropic material is significantly higher than that necessary in an isotropic material, which may have important implications when modeling the ductile fracture process.

1 INTRODUCTION

Fracture in ductile crystalline materials occurs via a process of void nucleation, growth and coalescence. Typically the voids, which are approximately spherical, nucleate from second-phase particles present in the material near a crack tip. The voids then grow under the influence of high stresses in the near crack tip region. Once the diameter of the voids has increased to a sufficiently large size, they coalesce either with the nearby crack tip or with neighboring voids. The microscale voids often are sufficiently small so that they exist entirely within a single grain of the polycrystalline material. Therefore it is important to account for the anisotropic constitutive properties of each individual grain to better understand void growth at the micron length scale.

An extensive literature on void growth in isotropic materials exists beginning with slip line theory solutions (e.g. [1]) and also elastic-plastic analyses for both cylindrical and spherical materials [2,3,4]. Very little work has been done to understand the effects of anisotropy on void growth. Numerical simulations of void growth in single crystals suggest that plastic anisotropy affects the growth of individual voids [5] by inducing non-axisymmetric displacement and stress fields. In addition, numerical simulations of the coalescence of neighboring voids in a crystal [6] show a pronounced dependence upon the crystallographic orientation of the void-containing material.

The stress and deformation fields around a cylindrical void in both face centered cubic and body centered cubic materials are presented herein. The solutions are developed by employing anisotropic slip line theory [7,8] which is valid for rigid-ideally plastic single crystals under plane strain conditions. The deformation state is divided into angular regions, called *slip sectors*, within which only one effective dislocation slip system is active. Each slip sector is further subdivided into smaller regions denominated *stress sectors* within which mathematical expressions for the prevailing stress state are valid. Complete details of the derivation for a void in a face centered

cubic material are presented in [9]. The derivation for a void in a body centered cubic material is similar. The analytical theory, experiments and finite element simulations all compare favorably.

2 GOVERNING EQUATIONS AND GEOMETRY OF VOID

Single crystals which deform plastically are clearly anisotropic in their behavior, which arises from the fact that plastic deformation occurs by the motion of dislocations within the crystal on discrete slip systems. The slip system of a dislocation is determined by the crystallographic plane (with unit normal \mathbf{n}) on which the dislocation exists as well as the direction of slip which the dislocation induces in the crystal (denoted by unit vector \mathbf{s}). The slip system is activated when the shear stress resolved onto the slip system in the direction of slip reaches a critical value, which is expressed mathematically for each system as $\mathbf{n} \cdot \boldsymbol{\sigma} \cdot \mathbf{s} = \pm \tau$, where τ is the experimentally determined critical resolved shear stress of the slip system and $\boldsymbol{\sigma}$ is the stress tensor.

If a line loading is applied parallel to a $\langle 110 \rangle$ direction in a face-centered cubic (FCC) or body-centered cubic (BCC) crystal, certain slip systems act cooperatively which enable plane strain conditions to be achieved. This is illustrated for FCC crystals in Figure 1a where the $\{111\}$ planes are shaded in gray and can be seen relative to the wire frame which corresponds to the external surfaces of the crystal; intersections of the $\{111\}$ planes correspond to $\langle 110 \rangle$ directions, which define the slip systems for FCC crystals. A line loading applied parallel to the $[110]$ direction in Figure 1a produces a plane strain deformation state in the $[\bar{1}10]$ – $[001]$ plane in Figure 1b made possible by three effective in-plane slip systems in the crystal. The effective plane strain slip systems consist of two slip systems which act cooperatively to achieve plastic slip only within the desired plane. The effective $(\bar{1}\bar{1}1)[\bar{1}12]$ slip system, which will be referred to as *slip system i*, is oriented at an in-plane angle of $\phi_1 = \tan^{-1} \sqrt{2} \approx 54.7^\circ$ counterclockwise relative to $[\bar{1}10]$ direction. The complex slip system acts in the $[\bar{1}10]$ direction, such that $\phi_2 = 0$, and will be referred to as *slip system ii*. The effective $(\bar{1}11)[1\bar{1}2]$ slip system is oriented at an in-plane angle of $\phi_1 = -\tan^{-1} \sqrt{2} \approx -54.7^\circ$ relative to the $[\bar{1}10]$ direction and will be referred to as *slip system iii*. The yield condition for each of the plane strain slip systems has a geometrical interpretation in the form of the yield surface in Figure 1c, which can be expressed mathematically as

$$\sigma_{12} = \tan 2\phi \left(\frac{\sigma_{11} - \sigma_{22}}{2} \right) \pm \frac{\beta\tau}{\cos 2\phi} \quad (1)$$

where β is a dimensionless term which relates the details of a slip system to the plane of plane strain [10] and for FCC crystals has values $\beta_1 = \beta_3 = 2/\sqrt{3}$ and $\beta_2 = \sqrt{3}$. The appropriate sign for β depends upon whether the slip system is activated in a positive or a negative sense. For what follows, we will assume that τ is unity. The values of β for BCC crystals are different from the FCC case which leads to somewhat different stress and deformation fields.

If eqn (1) is expressed in the polar coordinates (r, θ) , the yield condition can be rewritten

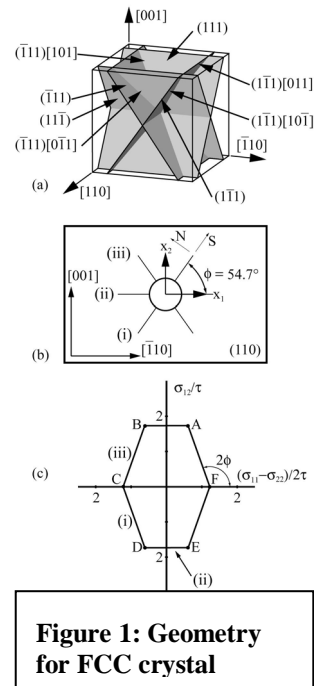


Figure 1: Geometry for FCC crystal

$$\sigma_{r\theta} = \tan[2(\phi - \theta)] \left(\frac{\sigma_{rr} - \sigma_{\theta\theta}}{2} \right) \pm \frac{\beta\tau}{\cos[2(\phi - \theta)]}. \quad (2)$$

Airy's stress function, Ψ , in polar coordinates can then be substituted into eqn (2) to obtain

$$\frac{1}{2} \sin[2(\phi - \theta)] \left(\frac{1}{r} \frac{\partial \Psi}{\partial r} + \frac{1}{r^2} \frac{\partial^2 \Psi}{\partial \theta^2} - \frac{\partial^2 \Psi}{\partial r^2} \right) - \cos[2(\phi - \theta)] \left(\frac{1}{r^2} \frac{\partial \Psi}{\partial \theta} - \frac{1}{r} \frac{\partial^2 \Psi}{\partial r \partial \theta} \right) \pm \beta\tau = 0 \quad (3)$$

which simultaneously satisfies equilibrium and the yield condition. It is a non-linear partial differential equation which is hyperbolic over its entire domain. Slip line plasticity theory satisfies equilibrium and the yield condition in a rigid-ideally plastic material undergoing plane strain deformation, while neglecting compatibility and the strain-displacement relations, so eqn (3) is an expression for slip line theory in a single crystal. The general slip line theory for an anisotropic material is well-developed [7,8] and will be used along with eqn (3) to derive the displacement and stress fields around the void.

3 BOUNDARY CONDITIONS AND ESTABLISHMENT OF SLIP SECTORS

Slip line theory addresses *incipient* plastic deformation so that boundary conditions can be applied to the material in its undeformed configuration. We assume that plastic deformation around the void is induced by a far-field loading and that zero traction boundary conditions hold on the void surface at $r = r_0$ so that $\sigma_{rr} = \sigma_{r\theta} = 0$. Further, as is required by slip line theory, we assume that the material is plastically deforming over the entire domain of interest. Therefore from eqn (2) the circumferential stress on the surface of the void is

$$\sigma_{\theta\theta} = \frac{\pm 2\beta\tau}{\sin[2(\phi - \theta)]} = \frac{2A}{\sin[2(\phi - \theta)]} \quad (4)$$

where $A = \pm\beta\tau$ and subscripts on A and ϕ will be used to designate particular slip systems.

In order to evaluate $\sigma_{\theta\theta}$ it is necessary to know which slip system is active. This can be determined from the geometry of the problem as in Figure 1b, where it is evident that the zero traction boundary conditions at the point where the x_1 -axis intersects the void surface require that $\sigma_{11} = \sigma_{12} = 0$ so the stress state lies on the abscissa of the yield surface. We will assume a compressive far-field stress state which implies that $\sigma_{\theta\theta} < 0$ at this point. Therefore the stress state must be at point F on the yield surface in Figure 1c so that both slip system i and slip system iii are active where the x_1 -axis intersects the void surface. If we now apply the same logic to Figure 2a where the x_1 -axis has been rotated counterclockwise relative to the crystallographic coordinate system, the zero traction boundary conditions require the stress state to lie somewhere between points F and A on the yield surface of Figure 2b. Therefore, single slip on slip system i is predicted where the x_1 -axis intersects the void surface. When the x_1 -axis rotates sufficiently so that the point A lies on the abscissa of the yield surface, the active slip system changes from i to ii . For the FCC crystal, this occurs when the x_1 -axis rotates counterclockwise $\gamma = \tan^{-1}(1/\sqrt{2}) \approx 35.3^\circ$. As the x_1 -axis continues to rotate, another transition from slip system ii to slip system iii occurs when the x_1 -axis has rotated counterclockwise $\phi_1 = \tan^{-1}(\sqrt{2}) \approx 54.7^\circ$. Slip system iii is active until the x_1 -axis has

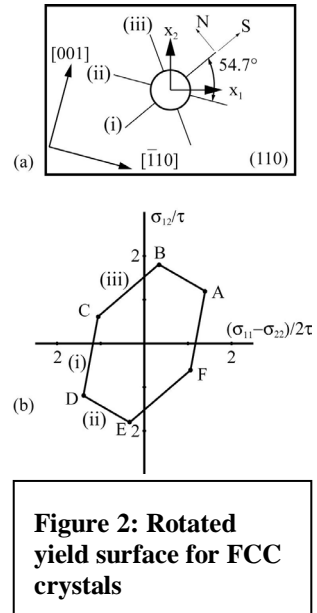


Figure 2: Rotated yield surface for FCC crystals

rotated counterclockwise by $\pi/2$, whereupon the deformation changes back to slip system i , and so on around.

Therefore, the deformation fields around the cylindrical void takes the form of angular sectors called *slip sectors*. Single slip conditions hold within each slip sector. The active slip systems on the void surface are illustrated in Figure 3, which also shows the profiles of the sector boundaries as they extend away from the void surface. The sector boundaries which are parallel and perpendicular to slip system ii are, by virtue of symmetry, radial lines with respect to the void. We can not make any statement yet about the shape of the other sector boundaries, which can be derived using anisotropic slip line theory, other than that they initiate at well-defined angles on the void surface. We will assume tentatively that the sector boundaries (which are regions of double slip) are vanishingly thin.

The slip sectors around a cylindrical void in a BCC crystal are different in two main ways. The angles at which the curved sector boundaries intersect the void surface are different from that of the FCC crystal. This leads to a slightly different shape of the curved sector boundaries.

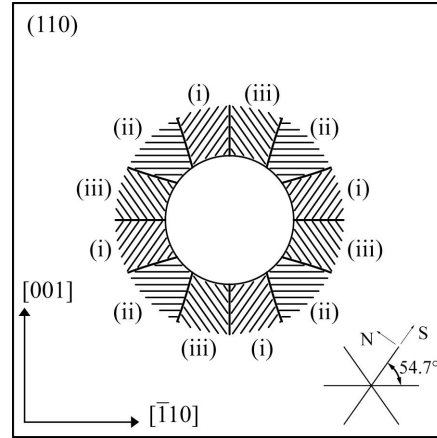


Figure 3: Slip sectors around void in FCC single crystal

4 ESTABLISHMENT OF STRESS SECTORS

Boundary conditions associated with hyperbolic partial differential equations often have only limited influence within the domain of a problem. Therefore, the region around the void must be broken into smaller sectors which are influenced by the zero traction boundary conditions. It can be shown that sectors I and II of Figure 4 are the only two regions around the void surface in which the stress state is determined solely by the zero traction boundary conditions. It is possible to find the solution for the Airy's stress function of eqn (3) for stress sectors I , II and III in Figure 4.

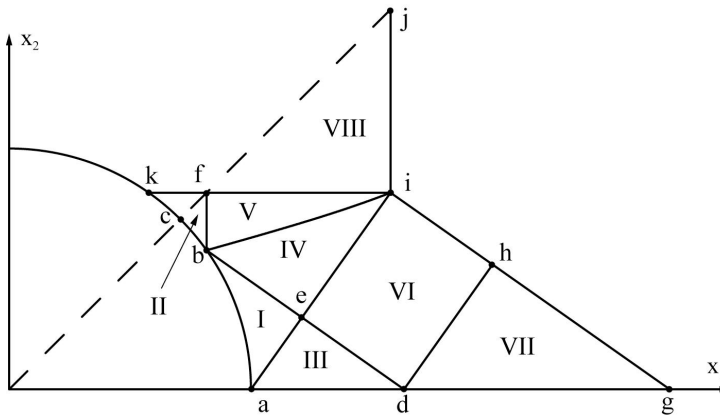


Figure 4: Stress sectors around a void in FCC crystal.

The stresses in the remaining sectors are found by recourse to various symmetry boundary conditions. The curved line bi in Figure 4 is the curved boundary between slip sector i and slip sector ii in the first quadrant of the void in Figure 3. The stresses in other quadrants around the void can be determined from symmetry.

5 STRESSES AROUND VOID

Three effective slip systems exist in the plane strain crystal, so there are six radial lines parallel to the slip systems which emanate from the center of the void as in Figure 1b; these will be referred to as *radial slip systems*. It is interesting to note that of the twelve slip sector boundaries around the circumference of the void, six of them intersect the void surface along a slip direction of one of the radial slip systems, and the other six intersect the void surface along a surface normal of one of the radial slip systems. The radial stresses, σ_{rr} , in Figure 5 exhibit a 12-point “star” structure, where each point reflects a slip sector boundary. Therefore the stress distribution around the void shows a clear dependence on the slip sectors and stress sectors. The circumferential stress, $\sigma_{\theta\theta}$, distribution is also influenced by the slip sector boundaries, but not as much as σ_{rr} . The polar shear stress, $\sigma_{r\theta}$, distribution exhibits a very complex nature within the confines of the crystal symmetries. It is interesting to note that the stresses around the void are continuous, however there are discontinuities of the stress gradient across the stress sector boundaries.

It is interesting to compare the in-plane pressure, defined as $\sigma = (\sigma_{rr} + \sigma_{\theta\theta})/2$, necessary to activate

plastic deformation around a void in an anisotropic material with that necessary for an isotropic material. For FCC crystals, at $r/r_0 = 1.2$ the value is $\sigma_{mean} = -2.04\tau$ and at $r/r_0 = 1.6$ the value is $\sigma_{mean} = -2.85\tau$. The in-plane pressure necessary to activate plastic deformation around a cylindrical void in an isotropic rigid-ideally plastic material (e.g. [1]) at $r/r_0 = 1.2$ is $\sigma_{mean} = -1.36\tau$ and at $r/r_0 = 1.6$ the value is $\sigma_{mean} = -1.94\tau$. Thus it is evident that a significantly larger mean pressure is required to achieve plastic deformation and growth of a void in an anisotropic material than in an isotropic material. This may have important implications when using concepts of void nucleation, growth and coalescence to model crack growth in ductile metals.

6 CONCLUSIONS

The anisotropic slip line theory solution was derived for a cylindrical void within FCC and BCC crystals. The governing non-linear hyperbolic partial differential equation in polar coordinates which satisfies equilibrium and constitutive relations appropriate for rigid-ideally plastic behavior

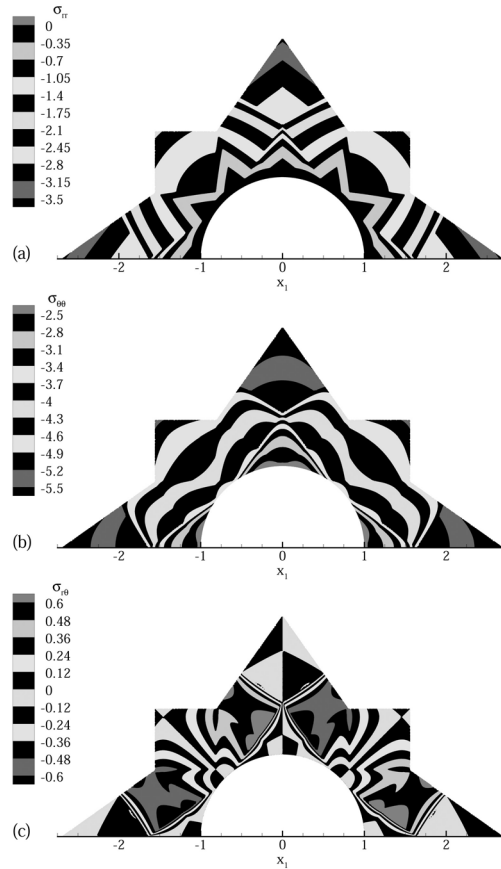


Figure 5: Polar stresses in FCC crystal

in a single crystal under plane strain conditions was derived in the form of an Airy's stress function. The associated characteristic lines of the governing equation were determined using the formalism of anisotropic slip line theory. Zero traction boundary conditions on the void surface require that the deformation fields take the form of angular sectors around the circumference of the void, within which only a single effective plane strain slip system is active. Within each sector of single slip, the domain is broken into smaller regions denominated stress sectors for which the stress state can be derived. The stresses are continuous around the void, however the stress gradients are discontinuous across the stress sector boundaries. The mean in-plane pressure necessary to activate plastic deformation around a void in an anisotropic material is significantly higher than that necessary for an isotropic material, which suggests that it is important to account for the anisotropy when modeling void growth and coalescence during ductile fracture. Full details of the derivation for the FCC crystal are given in [9].

ACKNOWLEDGEMENTS

Support from the National Science Foundation under the Faculty Early Career Development Program (CMS-0134226) is gratefully acknowledged.

REFERENCES

- [1] Kachanov, L.M., "Foundations of the theory of plasticity", North-Holland Pub. Co., Amsterdam, 1971.
- [2] Budiansky, B. and Mangasarian, O.L., "Plastic stress concentration at circular hole in infinite sheet subjected to equal biaxial tension", *Journal of Applied Mechanics*, **27**, 59-64, 1960.
- [3] Bishop, R. F., Hill, Rodney, Mott, N. F., "The theory of indentation and hardness tests", *Proceedings of the Physical Society*, **57**, 147-159, 1945.
- [4] Rice, J. R. and Tracey, D. M., "On the Ductile Enlargement of Voids in Triaxial Stress Fields", *Journal of the Mechanics and Physics of Solids*, **17**, 201-217, 1969.
- [5] O'Regan, T.L., Quinn, D. F., Howe, M.A., McHugh, P.E., "Void growth simulations in single crystals", *Computational Mechanics*, **20**, 115-121, 1997.
- [6] Schacht, T., Untermann, N., Steck, E., "The influence of crystallographic orientation on the deformation behaviour of single crystals containing microvoids", *International Journal of Plasticity*, **19**, 1605-1626, 2003.
- [7] Booker, J.R and Davis, E.H., "A general treatment of plastic anisotropy under conditions of plane strain", *Journal of the Mechanics and Physics of Solids*, **20**, 239-250, 1972.
- [8] Rice, J.R., "Plane strain slip line theory for anisotropic rigid-plastic materials", *Journal of the Mechanics and Physics of Solids*, **21**, 63-74, 1973.
- [9] Kysar, J.W., Gan, Y.X., Mendez-Arzuza, G., "Cylindrical Void in a Rigid-Ideally Plastic Single Crystal I: Anisotropic Slip Line Theory Solution for Face-Centered Cubic Crystals", *International Journal of Plasticity*, submitted.
- [10] Rice, J.R., "Tensile crack tip fields in elastic-ideally plastic crystals", *Mechanics of Materials*, **6**, 317-335, 1987.